

1                   **Gasification of low-grade SRF in air-blown fluidized bed:**  
2                   **permanent and inorganic gases characterization**

3                   Maxime Hervy<sup>1</sup>, Damien Remy<sup>1</sup>, Anthony Dufour<sup>1</sup>, Guillain Mauviel<sup>1\*</sup>

4  
5                   <sup>1</sup>LRGP, CNRS, Université de Lorraine, ENSIC, 1, Rue Grandville, Nancy, France

6                   Corresponding author: [guillain.mauviel@univ-lorraine.fr](mailto:guillain.mauviel@univ-lorraine.fr)

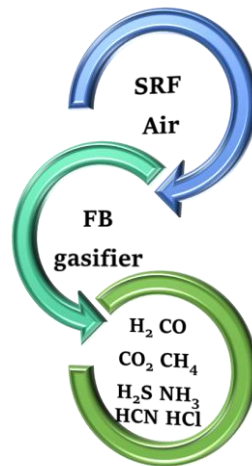
7  
8                   **Abstract**

9                   The influence of the gasification temperature and Equivalence Ratio (ER) on the behavior of  
10                  an industrial low-grade Solid Recovered Fuel (SRF) was investigated in an air bubbling  
11                  fluidized bed. The studied SRF exhibits an intermediate composition between biomass-rich  
12                  SRF and plastic-rich SRF. Its Lower Heating Value (14 MJ/kg) is low since its ash content is  
13                  very high (35 wt.%). But surprisingly, the Cold Gas Efficiency and the Carbon Conversion  
14                  were relatively high with this type of low-grade SRF. As a result, the syngas produced is quite  
15                  rich (LHV > 8 MJ/m<sup>3</sup> STP) and it may be valorized in gas engines. H<sub>2</sub>S, HCl, HCN and NH<sub>3</sub>  
16                  in the syngas were analyzed. These results confirm that inorganic gases are an important issue  
17                  for the valorization of SRF as fuel in gasification processes, even if significant parts of S, N  
18                  and Cl are not converted into inorganic gases.

19  
20                  **Keywords:** SRF; RDF; Gasification; Syngas; Inorganic



23 **Graphical abstract**



24

25 **Statement of Novelty**

26 This work is an original contribution that allows quantifying the different gas species that are  
27 obtained through SRF gasification in fluidized bed. These gas species include not only  
28 permanent gases, but also inorganic gases like H<sub>2</sub>S, NH<sub>3</sub>, HCN, HCl. These data are scarce in  
29 the scientific literature, whereas they are required in order to conceive a sustainable gasification  
30 process that will produce a purified syngas for CHP applications.

31

32 **Declarations**

33 **Funding:** the research was supported by ADEME through the project ADEME Terracotta n°  
34 1606C0013 led by EDF

35 **Conflicts of interest/Competing interests:** No conflict of interest

36 **Availability of data and material:** All the data published in these articles are available for  
37 the scientific community

38 **Code availability:** Not applicable

39

## 40 **1. Introduction**

41 The worldwide production of Municipal Solid Waste (MSW) is estimated around 2.01 billion  
42 tons per year, and around 70% of waste is disposed in landfill sites or openly dumped in natural  
43 sites [1]. This alarming situation creates catastrophic issues of air, soil, and water pollution  
44 affecting human health as well as flora and fauna life [2, 3]. It must prompt the society, starting  
45 with the scientific community, to react in order to improve and promote the collection, the  
46 recycling and the valorization of wastes [4–10]. While the most efficient solution would consist  
47 in the reduction of waste generation, this latter is unfortunately expected to increase to reach  
48 3.4 billion tons per year by 2050 [11]. Therefore, new efficient valorization routes must be  
49 developed.

50 Solid recovered fuels (SRFs) can be produced by sorting different waste streams and appear as  
51 one of the promising solutions to improve waste management [12]. SRFs consist of a mixture  
52 of different non-hazardous and non-recyclable solid waste fractions, such as plastics, textiles,  
53 tires, paper and carton, biomass waste, or sludge [13]. Consequently, SRFs are very complex  
54 and heterogeneous materials, and the proportion of each fraction can vary significantly  
55 depending on the waste origin, the season, the waste sorting plant, and the SRF production  
56 technique. SRFs represent a significant fuel resource, with a potential estimated at 70 million  
57 tons per year in Europe [14]. This resource represents 25-35 Mtep of primary energy, i.e.  
58 approximately 2 % of the consumption in Europe [15]. SRFs are complex heterogeneous fuels.  
59 Therefore, a rigorous definition of SRF characteristics is difficult to provide, which hinders the  
60 development of suitable valorization processes. Currently, SRFs are mainly used as a fuel in  
61 cement kiln, but other energetic valorizations are expected to be developed.

62 Thermochemical processes, such as incineration and gasification, are efficient ways for the  
63 management of municipal wastes [16, 17], as they allow the decomposition of contaminants

64 and the concentration of some inorganic species in the ashes [18]. In the gasification process,  
65 the solid fuel is partially oxidized at high temperature (800-1000 °C) using a gasifying agent  
66 (air, steam, O<sub>2</sub> or CO<sub>2</sub>). This process results in the production of syngas, composed of a mixture  
67 of H<sub>2</sub>, CO, CO<sub>2</sub>, CH<sub>4</sub>, and C<sub>n</sub>H<sub>m</sub> having high calorific value. One of the most important  
68 advantage of gasification over combustion is the different applications existing for the syngas.  
69 Depending on its purity, syngas can be used as a fuel in different power generator systems (gas  
70 engine, gas turbine, fuel cell), or as a precursor for gaseous fuels (H<sub>2</sub>, CH<sub>4</sub>) or liquid fuels  
71 synthesis [19, 20]. Different gasification technologies have been developed. Among them,  
72 fluidized bed reactor is the most adapted for waste valorization at medium-scale (1 to 100  
73 MW), due to the efficient flow mixing between reactants, the carefully controlled temperature,  
74 the high heat transfer performance, and the large operating flexibility. Indeed, fluidized bed  
75 reactor can be operated for the gasification of fuel having different properties [21, 22], such as  
76 meat waste and wastewater treatment sludge [23], tires [24, 25], poultry fuel [26], plastic  
77 wastes [27–29] etc. For this reason, fluidized bed gasifiers have been used in the past ten years  
78 for the gasification of SRFs [30, 31], these materials being very heterogeneous in terms of  
79 composition. The LHV of SRF can significantly vary depending on the waste origin and the  
80 SRF production method. The valorization of low-grade SRF by gasification process can be  
81 impeded if the syngas LHV is too low to be valorized in a gas engine. The presence of  
82 pollutants in the syngas (tar, inorganic gases, and particulate matter) also jeopardizes its  
83 valorization since it increases the syngas purification cost [32].

84 The pollutants content in syngas strongly depends on the gasification conditions and on the  
85 initial fuel composition [33]. For waste gasification, the tar content was proved to be slightly  
86 higher than for biomass gasification [30, 34–38]. For this reason, tar removal processes are  
87 required before valorizing syngas in gas engines. During waste gasification, the inorganic gases  
88 concentration can be significantly higher than that obtained in syngas from biomass due to the

89 high contents in nitrogen, chlorine, and sulphur species initially contained in the waste.  
90 Inorganic gases could lead to corrosion and clogging problems in the gasification process, to  
91 the poisoning of the catalysts used for syngas cleaning and upgrading, to acid rains [39–41],  
92 and also to combustion issue if syngas is burnt in a gas engine [42]. The main inorganic gases  
93 contained in syngas are H<sub>2</sub>S (100-30000 ppm), HCl (1-500 ppm), NH<sub>3</sub> (500-14000 ppm) and  
94 HCN [32, 43–47]. Their content must be drastically reduced to reach the standards required for  
95 syngas valorization. For this reason, the measurement of the inorganic gases concentration in  
96 syngas from SRF must be accurately carried out.

97 In the literature, different methods have been explored to analyze inorganic gases in syngas.  
98 Most of them consists in the absorption of inorganic gases in impingers filled with different  
99 solutions which are then analyzed. The composition of the absorbing solutions as well as the  
100 analytical tools are different in the studies reported in the literature [31, 48–51]. Indeed, H<sub>2</sub>S,  
101 NH<sub>3</sub>, HCN and HCl after absorption and under ionic state can be analyzed by ion  
102 chromatography, potentiometry, iodometry, ion electrophoresis, or indophenols blue  
103 absorption spectrophotometry [52]. Syngas can be analyzed on-line (by IR based spectroscopy)  
104 but these methods are hardly quantitative due to important artefacts coming from H<sub>2</sub>O and CO<sub>2</sub>.  
105 Sulphur gases can also be directly analyzed by gas chromatography equipped with a PoraPLOT  
106 U column and Thermal Conductivity Detector (TCD), but this technique suffers from relatively  
107 high detection limit (around 1 ppm) [52, 53] which is typically too high to analyze the syngas  
108 purity after the syngas cleaning operations. Pulse Flame Photometer Detector (PFPD) are  
109 efficient detectors to analyze inorganic gases, but hydrocarbon species in syngas must be  
110 quenched prior to analysis [52]. Recently, new techniques have been developed to analyze S  
111 species in syngas of biogas, such as Optical Feedback Cavity-Enhanced Absorption  
112 Spectroscopy (OF-CEAS), or ion-molecule reactions-mass spectrometry (IMR-MS) [52].

113 While the decrease in tar concentration with increasing Equivalence Ratio (ER) and  
114 gasification temperature was unanimously reported [54, 55], the evolution of inorganic gases  
115 with operating conditions in bubbling fluidized bed is currently discussed in the literature.

116 First, concerning the effect of reactor temperature, a temperature rise was proved to increase  
117 the release of HCN, while  $\text{NH}_3$  decreased [30, 50, 54]. The nature of the solid N-compounds  
118 strongly influences the release of nitrogenous species. In carbonaceous materials, different  
119 nitrogen groups can be present: pyrrole, pyridine, pyridinium, pyridine oxide, amine, nitro,  
120 nitroso, and cyano compounds [56].  $\text{NH}_3$  results from the decomposition of amino-groups,  
121 whereas HCN mainly originates from the decomposition of pyrrolic and pyridinic nitrogen  
122 [57–60]. As SRFs may be rich in plastics, the gasification performed at relatively high heating  
123 rate was proved to promote the release of HCN [61]. While part of the nitrogenous compounds  
124 can be in the form of tar [62] and char [63] after pyrolysis, secondary reactions can transform  
125 these nitrogenous compounds into HCN during gasification [64]. In addition, the drop of  $\text{NH}_3$   
126 release with increasing temperature can be attributed to the thermal decomposition of  $\text{NH}_3$  into  
127  $\text{N}_2$  [65]. This reaction can be catalyzed by the presence of calcium, potassium and iron in the  
128 SRF ashes [66]. The HCl content drastically drops with rising temperature [30, 50]. Chlorine  
129 in SRF could originate from both organic (PVC) and inorganic (salts) sources [67] which are  
130 partially decomposed in the form of HCl during gasification. The decrease of HCl in the gas  
131 phase with rising temperature is explained by the presence of alkali metals (especially K).  
132 Indeed, at low temperature ( $<700\text{ }^\circ\text{C}$ ), alkali species are mainly in the form of alkaline  
133 carboxylates. These structures decompose at higher temperature, and alkali metals are then  
134 available to react with HCl, which decreases the HCl content in gas phase [68–70]. However,  
135 the presence of silica and sulfur in the fuel was proved to increase the HCl formation [67].  
136 Sulfur contained in SRF originates from organic and inorganic sources, and elastomers (such  
137 as rubber) represent an important input [14].  $\text{H}_2\text{S}$  is the main S-containing gas released during

138 gasification [47, 71]. A temperature rise was proved to increase the release of H<sub>2</sub>S [38, 50, 54].  
139 While organic sulfur is decomposed at low temperature (around 500°C) [72], inorganic sulfates  
140 in the chars have higher binding energy and are decomposed at higher temperature [73]. Thus,  
141 when the temperature increases, higher amount of H<sub>2</sub>S is released. Besides, some inorganic  
142 species (such as Ca, K or Fe) can react with H<sub>2</sub>S to form sulfides and immobilized sulfur in the  
143 solid phase, thus decreasing the H<sub>2</sub>S release [73, 74]. Nevertheless, *Pinto et al.* observed no  
144 effect of temperature on the release of H<sub>2</sub>S during the gasification of SRF [31].

145 Second, the influence of the ER on the release of inorganic gases in allothermal gasification  
146 reactors is a controversial topic in the literature. The release of inorganic gases could be  
147 expected to increase as ER rises, since the secondary reactions (char gasification, tar reforming)  
148 could be promoted by oxidation reactions thus favoring the release of Cl, N or S. *Pinto et al.*  
149 showed that the ratio of sulphur converted into H<sub>2</sub>S to the amount of S in the feedstock  
150 increased with increasing ER [31]. It has been reported that the NH<sub>3</sub> concentration increases  
151 with rising ER [31, 49]. However, several studies showed that the concentration of inorganic  
152 gases (H<sub>2</sub>S, HCl, HCN, NH<sub>3</sub>) in the syngas decreases with rising ER [50, 54, 75]. This trend  
153 can be explained by the promotion of char gasification reactions which promote the contact  
154 and reactions between inorganic gases and the mineral species of the ash (Fe, Ca, K, Na)  
155 resulting in the immobilization of Cl, N or S atoms in the ashes. This decrease can also be  
156 attributed to oxidation reactions promoting the formation of SO<sub>x</sub> and NO<sub>x</sub> [50]. In addition, the  
157 decrease in inorganic gases concentration can result from a dilution effect due to the ER  
158 increase. Indeed, when the ER is increased in an air fluidized bed process, the syngas produced  
159 is diluted in a larger amount by nitrogen, thus decreasing the inorganic gases concentration.  
160 Rigorous measurements must be performed to better understand the distribution of S, Cl, and  
161 N.



162 These apparent discrepancies in literature results could be attributed both to the composition  
163 of the SRFs studied and to the nature of the bed material. Indeed, the nature of the bed material  
164 plays a significant role in the release of inorganic gases. *Pinto et al.* showed that dolomite, lime  
165 and olivine allowed to decrease the H<sub>2</sub>S content in the syngas [31]. The more reactive materials  
166 were dolomite, lime, and finally olivine. This reactivity was attributed to the formation of  
167 sulfides by reactions between H<sub>2</sub>S and Ca (in dolomite and lime), and to the presence of Fe in  
168 olivine. Contradictory results were reported in the literature on the effect of natural minerals  
169 on the NH<sub>3</sub> release. Some study highlighted the reduction of NH<sub>3</sub> release with natural minerals  
170 [76], while other showed that it increased as these materials catalyzed the char gasification  
171 reactions thus promoting the release of heteroatoms [31]. The type of reactor wall, as well as  
172 the sampling and analyzing methods were also proved to influence the measurement of  
173 inorganic gases [77].

174 Despite all these previous studies, the effect of temperature and ER on the fate of S, Cl, and N  
175 species remains unclear.

176 For this reason, the present study investigates the air gasification of an industrial SRF in a  
177 fluidized bed. Olivine was used as a common and cheap bed material. At industrial scale, the  
178 gasifiers are autothermal, while the reactor walls have to be heated at lab-scale to balance heat  
179 losses. Thus, it has been possible to study the respective effects of temperature and ER on the  
180 gasification efficiency by varying these two parameters independently. Gasification efficiency  
181 was evaluated based on four indicators: cold gas efficiency (CGE), carbon conversion (CC),  
182 syngas lower heating value (LHV<sub>syngas</sub>), and the syngas yield ( $\eta_{\text{syngas}}$ ). A previous article has  
183 presented the effect of gasification conditions on these 4 indicators for two SRFs (one rich in  
184 biomass and glass, and a second richer in plastics) [78]. The present article supplements this  
185 previous study with another SRF which exhibits an interesting composition between biomass-  
186 rich SRF and plastic-rich SRF. Therefore, this SRF presents a complex gasification behavior

187 of high interest for the waste management community. In order to better characterize its  
188 gasification behavior, the analysis of the inorganic gases is reported in this study.

189 **2. Materials and methods**

190 **2.1 Characterization of the Solid Recovered Fuel and Fly Ashes**

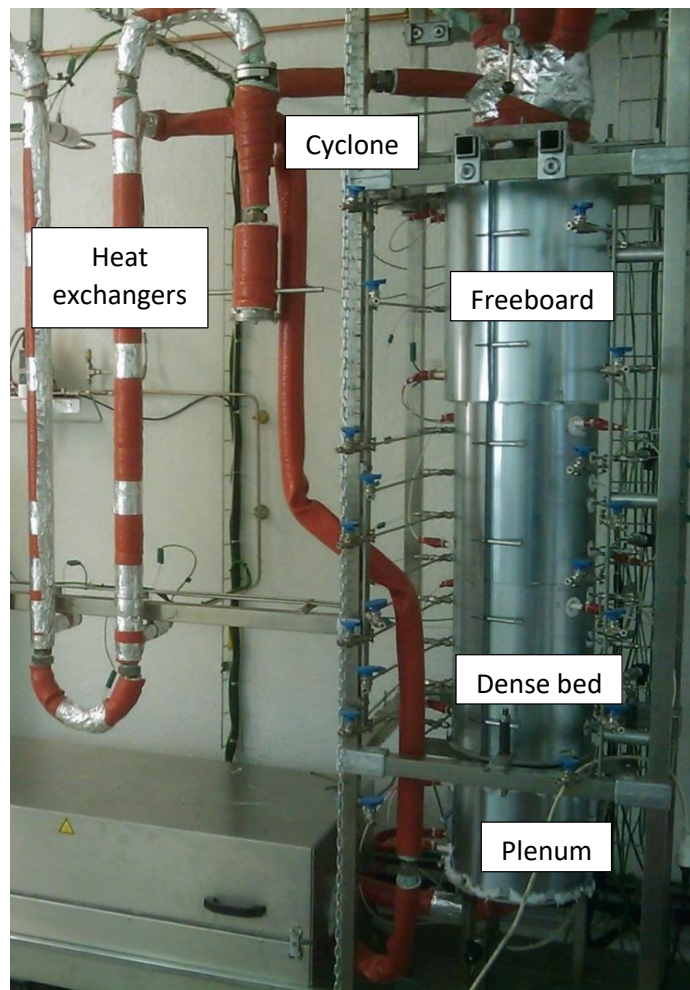
191 The SRF studied was provided by a French company of waste management and valorization.  
192 It was selected as its composition was intermediate between biomass-rich SRF and plastic-rich  
193 SRF. The same characterization methods were used for this SRF and for the Fly ashes  
194 recovered in the cyclone after the experiments. The elemental composition was measured  
195 according to the standard NF EN 15407. The ash content was measured at 550°C according to  
196 the standard NF EN 15403. The composition of the resulting ashes was measured by X-Ray  
197 Fluorescence Spectroscopy. Inductively Coupled Plasma – Atomic Emission Spectroscopy  
198 (ICP-AES) was also used to characterize the mineral composition of the ashes after ash melting  
199 (NF-M03-042). The SRF sample was calcined at 815°C, and the remaining ashes were melted  
200 with  $\text{Li}_2\text{B}_4\text{O}_7$  at 1000°C, before being dissolved in hydrochloric acid solution and detected by  
201 AES detector. Finally, ionic chromatography was used to analyze the halogen compounds (NF  
202 EN 1548 and NF EN ISO 10304-1).

203 The Lower Heating Value (LHV) of the SRF was measured with a calorimetric bomb (NF EN  
204 15400). The proportion and composition of biomass, non-biomass, and inert materials were  
205 determined according to the standard NF EN 15440 that is based on manual sorting.

206

207 **2.2 Gasification reactor and analysis of gas**

208 Gasification tests were performed in a bubbling fluidized-bed constructed at CNRS Nancy and  
209 made of stainless steel 310 (Figure 1) [36, 78]. Briefly the gasifier is divided into three zones:  
210 the plenum (d=100 mm, H=300 mm), the bed zone (d=100 mm, H=800 mm), and the freeboard  
211 zone (d=140 mm, H=800 mm). The gasifying agent was air whose flow rate was controlled by  
212 a mass flow controller (Brooks 5850S). At the bottom of the gasifier, a 3mm thick inox grid  
213 was used as distributor plate to homogenize the air flow and insure an efficient fluidization.  
214 The gasifier is heated by eight electrical heater shells at a maximum temperature of 1000 °C.



215

216

**Fig. 1** Picture of the gasification unit

217 SRF were fed at the top of the reactor with a sloping screw. Around 3 kg of olivine was placed  
218 in the gasifier. At 800°C, the minimum fluidization velocity ( $U_{mf}$ ) was 0.15 m/s as measured  
219 in this reactor by progressively increasing the air flowrate while measuring the pressure drop  
220 in the gasifier (without SRF injection). This  $U_{mf}$  is in agreement with Cluet et al. [79]. At the  
221 gasifier outlet, the syngas flowed through a cyclone to remove particles, before to be cooled  
222 with two air heat exchangers. A water Venturi scrubber was also used to remove the tars and  
223 the inorganic gases before flaring the syngas. The gasifier is equipped with 19 lateral tubes  
224 allowing to insert thermocouples which locally measure the bed and freeboard temperatures.  
225 Pressure was continuously measured below the grid and at the top of the freeboard zone.

226 The syngas was sampled before the Venturi scrubber and analyzed on-line by a  $\mu$ -GC (Varian  
227 micro-GC 490, 4 modules) every 3 minutes.  $N_2$ , CO,  $CO_2$ ,  $H_2$ ,  $CH_4$ ,  $C_2H_2$ ,  $C_2H_4$ ,  $C_2H_6$ ,  $C_3H_4$ ,  
228  $C_3H_6$ , and  $C_6H_6$  were quantified with this technique. To quantify the inorganic gases ( $H_2S$ ,  
229 HCN, HCl and  $NH_3$ ) present in syngas, the sampling procedure has been adapted from previous  
230 articles [51, 54]. The analysis of the solutions was performed according to French and ISO  
231 standards. 10 L of syngas was sampled in a Tedlar bag at the exit of the first heat exchanger.  
232 Then, the syngas sampled in Tedlar bag was sequentially flowed at a constant flowrate (400  
233 mL/min) during 5 minutes in impingers filled with 200 mL of specific solutions ([Table S.1 in](#)  
234 [Supplementary Material](#)). The targeted ions  $S^{2-}$  (representing  $H_2S$ ),  $Cl^-$  (representing HCl), and  
235  $NH_4^+$  (representing  $NH_3$ ) were analyzed by spectrophotometry, while the ion  $CN^-$  (representing  
236 HCN) was quantified by ionic chromatography ([Table S.1 in Supplementary Material](#)).

### 237 238 [2.3 Gasification experimental protocol & performance indicators](#)

239 Before starting the gasification tests, the system was preheated at the desired temperature (750-  
240 900 °C) under air. When the temperature was at the target value, the air flowrate was set at the  
241 desired value. For all experiments, the air velocity was set at 4 times the minimum fluidization

242 velocity (thus 0.6 m/s), corresponding to an air flow rate of 4.5 m<sup>3</sup>/h (STP). Once the  
243 temperatures were stable along the gasifier, the feeding of the SRF was started at a controlled  
244 flowrate to reach the targeted equivalence ratio (ER). When the gasification conditions were  
245 stable (gasifier temperature, and syngas composition analyzed by  $\mu$ -GC), the steady-state  
246 regime was maintained at least 40 minutes (Figure S.1 in supplementary material).

247 The ER is defined as the operating air flow rate divided by the air flow rate required for the  
248 stoichiometric oxidation of SRF. In this study, the ER was varied between 0.18 and 0.27. The  
249 effect of the ER on the gasification efficiency was studied at 800 °C (controlled by electrical  
250 heater shells). To do so, the SRF flowrate was adjusted (between 4.67 to 6.95 kg/h) while the  
251 air flow rate and the bed temperature were kept constant. In these conditions, the gas velocity  
252 and residence time were similar for the different gasifying conditions. The SRF flow rate was  
253 found to fluctuate by +/- 10% over time. For this reason, the ER range for each experimental  
254 condition is presented in the results section. The SRF tank was continuously flushed with 10  
255 L/min (STP) of pure N<sub>2</sub> to avoid the conversion of the fuel in the feeding screw. This flow rate  
256 was taken into consideration for the results analysis since N<sub>2</sub> is used as a tracer for the  
257 calculation of the syngas flowrate.

258 Four indicators of the gasification performance were used, namely: lower heating value of the  
259 dry syngas (LHV<sub>syngas</sub>), syngas yield ( $\eta_{\text{syngas}}$ ), carbon conversion (CC), Cold Gas Efficiency  
260 (CGE). Their determination based on experimental analysis was presented in a previous article  
261 [78]. In these calculations, all the light hydrocarbon species (including benzene) were  
262 considered as syngas components since their presence is not an issue for syngas valorization in  
263 gas engine.

264 The lower heating value of the dry syngas (LHV<sub>syngas</sub>), expressed in MJ/m<sup>3</sup> (STP) of syngas  
265 (including N<sub>2</sub>), is calculated according to Eq.1:

$$266 \quad \text{LHV}_{\text{syngas}} = \frac{\sum_i (x_i \text{LHV}_i)}{V_m} \quad \text{Eq.(1)}$$

267 Where  $V_m$  is the molar volume of ideal gas at STP (22.4 L/mol), and  $x_i$  the molar fraction of  
 268 the gas species  $i$ .

269 The syngas yield ( $\eta_{\text{syngas}}$ ) is calculated as the volume of dry syngas produced (including  $\text{N}_2$ ) by  
 270 kg of SRF (on dry ash free basis):

$$271 \quad \eta_{\text{syngas}} = \frac{Q_{V_{\text{syngas}}}}{Q_{m_{\text{SRF}}}} \quad \text{Eq.(2)}$$

272 Where  $Q_{V_{\text{syngas}}}$  is the volumetric syngas flowrate including  $\text{N}_2$  ( $\text{m}^3/\text{h}$  STP) which is calculated  
 273 using  $\text{N}_2$  as a tracer, and  $Q_{m_{\text{SRF}}}$  the mass flowrate of SRF ( $\text{kg}_{\text{daf}}/\text{h}$ ).

274 The carbon conversion (CC) corresponds to the percentage of carbon transferred from SRF to  
 275 syngas:

$$276 \quad \text{CC} = Q_{m_{\text{syngas}}} M_C \frac{\sum_i \left( \frac{\omega_i}{M_i} n_i^C \right)}{Q_{m_{\text{SRF}}} X_C^{\text{SRF}}} \times 100 \quad \text{Eq.(3)}$$

277 Where  $Q_{m_{\text{syngas}}}$  is the mass flowrate of syngas ( $\text{kg}/\text{h}$ ),  $M_C$  is the molecular weight of carbon,  
 278  $n_i^C$  is the number of carbon atoms in the molecule  $i$ ,  $X_C^{\text{SRF}}$  is the mass fraction of carbon in SRF  
 279 (on daf basis), and  $\omega_i$  and  $M_i$  correspond to the mass fraction of the gas  $i$  in the syngas and its  
 280 molecular weight, respectively

281 Finally, the last indicator is the Cold Gas Efficiency (CGE) which reflects the fraction of  
 282 chemical energy transferred from SRF to syngas:

$$283 \quad \text{CGE} = \frac{\eta_{\text{syngas}} \text{LHV}_{\text{syngas}}}{\text{LHV}_{\text{SRF}}} \times 100 \quad \text{Eq.(4)}$$

284 In addition, the distribution of H atoms and C atoms in the gaseous products was calculated,  
 285 according to Eq.(5) and (6):

$$286 \quad S_H^i = \frac{n_H^i F^i}{\sum_k (n_H^k F^k)} \quad \text{Eq.(5)}$$

$$287 \quad S_C^i = \frac{n_C^i F^i}{\sum_k (n_C^k F^k)} \quad \text{Eq.(6)}$$

288 Where  $S_H^i$  and  $S_C^i$  are the molar selectivity representing the molar flow rate of H (resp. C) atoms  
289 present in a given molecule divided by the total flow rate of H (resp. C) atoms present in all  
290 syngas molecules.  $F^i$  is the molar flowrate of a given molecule i.



291 **3. Results and discussion**

292 **3.1 Physico-chemical properties of the SRF**

293 The elemental composition of SRF is presented in **Table 1**. The carbon content is relatively low  
294 (36.6 wt.%) while the ash content (35.1 wt.%) is significant compared to other SRFs reported  
295 in the literature. Indeed, the carbon content usually ranges from 41 to 84 wt.% while the ash  
296 content is in the range 1-27 wt.% [28, 30, 34, 48, 50, 54, 55, 80]. This composition results from  
297 the production of SRF by mechanical-biological treatment of municipal solid waste. On the  
298 contrary, the oxygen and hydrogen contents of this SRF are relatively lower than the reported  
299 values. Mainly due to its high ash content, the LHV of the SRF (14.1 MJ/kg) is lower than the  
300 values reported in the literature for SRFs (15-35 MJ/kg).

301 **Table 1** Elemental analysis and lower heating value of the SRF

<b>Elemental analysis (dry wt.%)</b>	
<b>C</b>	36.6
<b>H</b>	4.6
<b>N</b>	1.9
<b>S</b>	0.8
<b>O (by difference)</b>	21.1
<b>Ash</b>	35.1
<b>LHV (MJ/kg<sub>dry</sub>)</b>	14.1

302

303 The ash composition of the SRF is presented in **Table 2**. The main inorganic species are Si, Ca,  
304 and Al. Alkaline and alkaline earth metals (AAEM, such as Mg, Na, K) are also present in the  
305 ash composition. Some differences appear between ICP and XRF analysis. The SiO<sub>2</sub>, Fe<sub>2</sub>O<sub>3</sub>,  
306 and MnO contents are higher with ICP-AES measurement, while the CaO, TiO<sub>2</sub>, and Na<sub>2</sub>O<sub>3</sub>  
307 contents were higher with XRF analysis. ICP and XRF give similar values for Al<sub>2</sub>O<sub>3</sub>, MgO,  
308 SO<sub>3</sub>, P<sub>2</sub>O<sub>5</sub>. These results suggest that the characterization of complex wastes such as SRF must  
309 be carefully performed and slight differences can be measured despite a rigorous sampling

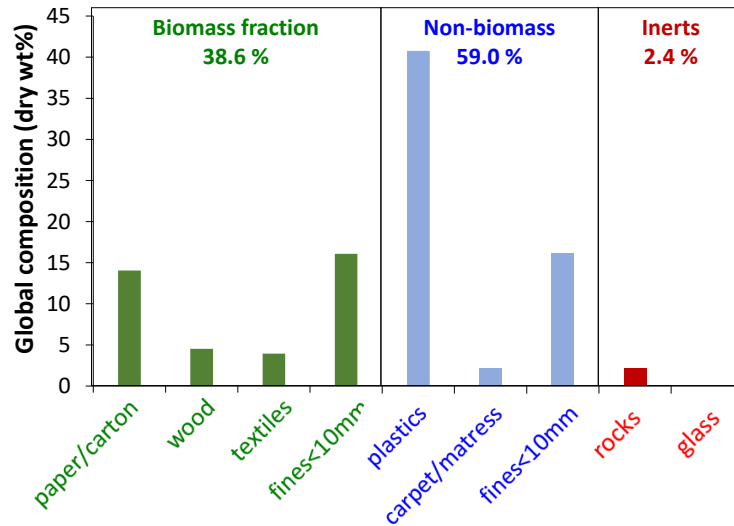
310 methodology. Regarding the potential inorganic gases release, it can be noted that the nitrogen  
 311 and chlorine contents are lower than that of other SRFs studied in the literature (0.2-1.3 wt.%  
 312 for N, and 0.7-1.1 wt.% for Cl) [30, 50, 54], whereas the sulphur content is slightly higher than  
 313 the values reported in the literature (0-0.6 wt.%) [30, 31, 34, 48, 50, 54, 55].

314 **Table 2** Ash composition of the SRF measured by ICP-AES and XRF

<b>Ash composition (in wt.%)</b>		
	ICP-AES	XRF
<b>SiO<sub>2</sub></b>	41.5	30.8
<b>Al<sub>2</sub>O<sub>3</sub></b>	10.5	10.5
<b>Fe<sub>2</sub>O<sub>3</sub></b>	4.1	2.6
<b>TiO<sub>2</sub></b>	1.1	1.8
<b>CaO</b>	24.0	34.6
<b>MgO</b>	4.2	4.0
<b>Na<sub>2</sub>O</b>	2.6	3.3
<b>K<sub>2</sub>O</b>	0.9	0.5
<b>SO<sub>3</sub></b>	9.8	10.6
<b>P<sub>2</sub>O<sub>5</sub></b>	1.0	1.0
<b>MnO</b>	0.2	0.1
<b>Total</b>	100.0	100.0
<b>Br</b>	<i>nd</i>	
<b>Cl</b>	0.30	
<b>F</b>	0.04	

315 **Figure 2** shows the proportion and composition of biomass, non-biomass, and inert fractions  
 316 composing the SRF. Our previous article presented the effect of operating conditions on  
 317 gasification efficiency for two SRFs (one rich in biomass and glass, and a second richer in  
 318 plastics) [78]. Herein we complete our previous study with another SRF which exhibits an  
 319 interesting composition between biomass-rich SRF and plastic-rich SRF. Indeed, this sample  
 320 is composed of non-biomass (59.0 wt.%), biomass (38.6 wt.%), and inert (2.4 wt.%) fractions.  
 321 The non-biomass fraction is rich in plastics, while the biomass fraction is mainly composed of  
 322 paper/carton. Significant parts of these fractions are composed of fines for which the origin has  
 323 not been identified and that may contain ash-rich materials. This would explain the high ash  
 324 content of this SRF (35.1 wt.%), whereas the inert fraction is low (2.4 wt.%). This inert fraction

325 is only composed of rocks (not glass). It must be noted that the SRF composition strongly  
 326 depends on the origin of the collected wastes and on the sorting methods used by the waste  
 327 treatment plant.



328

329 **Fig. 2** Proportion and composition of biomass, non-biomass, and inert materials in the SRF

330 **3.2 Permanent gases composition**

331 **3.2.1 Influence of the temperature**

332 The values of the cold gas efficiency (CGE), the carbon conversion (CC), the syngas yield  
 333 ( $\eta_{\text{syngas}}$ ) and the lower heating value of the syngas ( $\text{LHV}_{\text{syngas}}$ ) obtained during the gasification  
 334 tests are presented in **Table 3**. It can be noted that the temperature increase from 750 to 800 °C  
 335 does not significantly modify the gasification results. However, at 900 °C, all the gasification  
 336 indicators are strongly improved. The combined increase in  $\text{LHV}_{\text{syngas}}$  (+4.5%) and  $\eta_{\text{syngas}}$   
 337 (+10%) result in an overall gain of 13% for the CGE (from 74.5 to 84.3 %). The temperature  
 338 increase also promotes the carbon conversion (+6%). Some explanations are given thereafter.

339

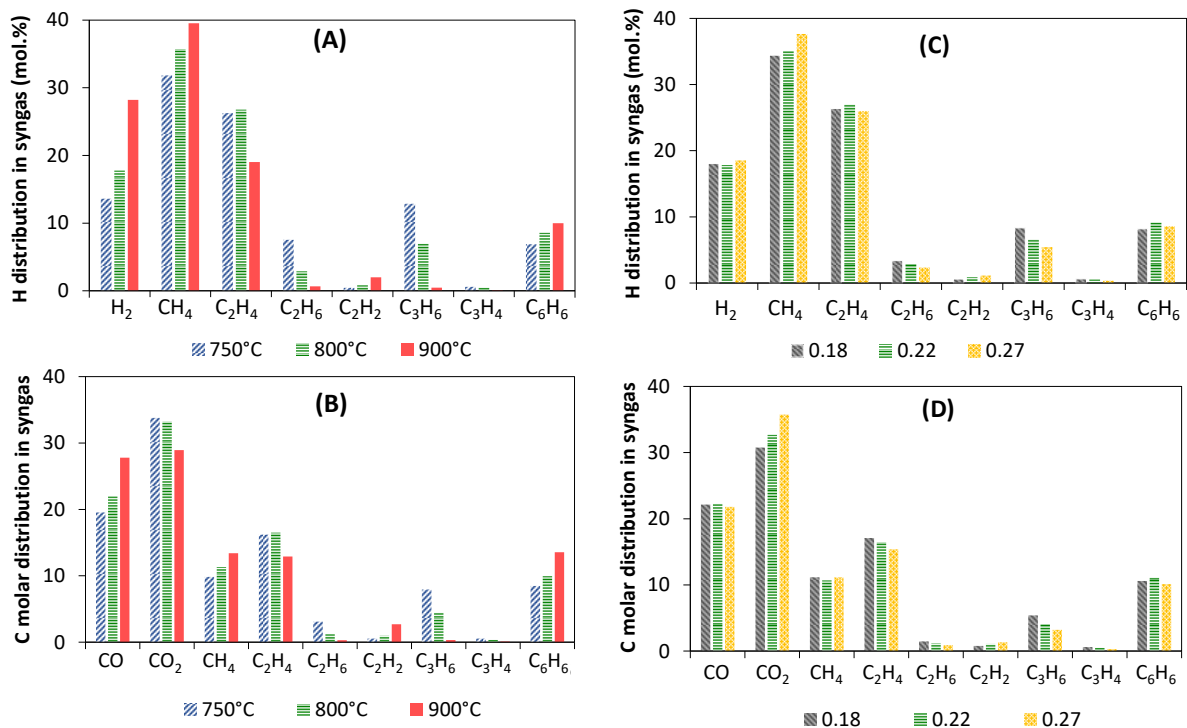
340 **Table 3** Operating conditions and results of the gasification tests performed at different  
 341 temperatures and ER=0.22 (ranging between 0.205 and 0.227), and at different Equivalent  
 342 Ratio (ER) and a Temperature of 803°C

T (°C)	Influence of T			Influence of ER		
	750	803	902	803	803	803
<b>Equivalence Ratio</b>	0.22 (0.205- 0.227)	0.22 (0.205- 0.227)	0.22 (0.205- 0.227)	0.18 (0.170- 0.188)	0.22 (0.205- 0.227)	0.27 (0.253- 0.279)
<b>Syngas composition (%vol.)</b>						
<b>N<sub>2</sub></b>	59.6	57.7	54.1	53.7	57.7	63.0
<b>H<sub>2</sub></b>	4.0	5.0	8.7	5.8	5.0	4.5
<b>CO</b>	9.3	10.3	12.6	11.0	10.3	8.8
<b>CO<sub>2</sub></b>	16.0	15.1	13.2	15.2	15.1	14.5
<b>CH<sub>4</sub></b>	4.7	4.9	6.1	5.5	4.9	4.5
<b>C<sub>2</sub>H<sub>4</sub></b>	3.8	3.8	2.9	4.2	3.8	3.1
<b>C<sub>2</sub>H<sub>6</sub></b>	0.7	0.3	0.1	0.4	0.3	0.2
<b>C<sub>2</sub>H<sub>2</sub></b>	0.1	0.3	0.6	0.2	0.3	0.3
<b>C<sub>3</sub>H<sub>6</sub></b>	1.3	0.6	0.1	0.9	0.6	0.4
<b>C<sub>3</sub>H<sub>4</sub></b>	0.1	0.1	0.0	0.1	0.1	0.0
<b>C<sub>6</sub>H<sub>6</sub></b>	0.7	0.9	1.0	0.9	0.9	0.7
<b>LHV<sub>syngas</sub> (MJ/m<sup>3</sup> STP)</b>	7.97	8.05	8.38	9.1	8.05	6.7
<b>η<sub>syngas</sub> (m<sup>3</sup> STP/kg<sub>SRF</sub> daf)</b>	2.00	2.06	2.20	1.84	2.06	2.33
<b>Carbon conversion (%)</b>	88.4	90.3	94.9	86.7	90.3	89.9
<b>Cold Gas Efficiency (%)</b>	73.0	76.2	84.3	77.0	76.2	71.7

343 In the literature, similar trends were reported, where rising gasification temperature at constant  
 344 ER promoted the syngas yield and carbon conversion[38]. However, a significant discrepancy  
 345 was reported in the literature for the evolution of CGE and LHV<sub>syngas</sub>, since they were reported  
 346 to decrease with increasing temperature [50, 54]. It has to be stressed out that, at industrial  
 347 scale, such a temperature rise in the gasifier is obtained by increasing the ER resulting in higher  
 348 syngas oxidation. In our case, ER is varied by maintaining a constant temperature thanks to the  
 349 heating of the reactor walls.

350 The evolution of the syngas composition (Table 3) explains the increase in calorific value with  
351 rising temperature. Indeed, H<sub>2</sub>, CO, CH<sub>4</sub>, C<sub>2</sub>H<sub>2</sub>, and C<sub>6</sub>H<sub>6</sub> contents significantly increase at 900  
352 °C, while CO<sub>2</sub> is substantially reduced. High temperature is known to promote char gasification  
353 reaction leading to the production of H<sub>2</sub> and CO [78]. H<sub>2</sub> and CO formation at elevated  
354 temperature can also result from tar decomposition by cracking, as well as steam and dry  
355 reforming [30, 50, 54]. Dry reforming reaction can contribute to the decrease of CO<sub>2</sub> with  
356 increasing temperature. This set of reactions is responsible for the evolution of syngas  
357 composition and gasification efficiency with rising temperature.

358 It can be highlighted that, despite the high ash content, no melting phenomenon leading to bed  
359 defluidization and agglomeration were observed under these operating conditions. Compared  
360 with syngas produced by miscanthus air gasification in the same reactor under similar operating  
361 conditions [36], the syngas produced in this study has lower content of H<sub>2</sub> and CO, while the  
362 content in CH<sub>4</sub> and small hydrocarbon compounds (especially C<sub>2</sub>H<sub>4</sub>) is significantly higher.  
363 This high content in hydrocarbon compounds is explained by the presence of plastics which  
364 are known to produce high content in CH<sub>4</sub> and C<sub>2</sub>-C<sub>3</sub> compounds during gasification [48, 55,  
365 78].



366

367

**Fig. 3** Distribution of hydrogen and carbon atoms in syngas species as function of

368

gasification temperature on (A) and (B), and of ER on (C) and (D).

369

The influence of the temperature on the distribution of hydrogen and carbon atoms in the

370

gaseous products is presented in Figure 3-A and B, respectively. The main H-containing

371

species is CH<sub>4</sub> (Figure 3-A), resulting from the decomposition of tar compounds [81–83].

372

Rising temperature increases the selectivity in H<sub>2</sub>, especially at temperature higher than 800

373

°C. At the same time, the selectivity in light hydrocarbons (C<sub>2</sub>H<sub>4</sub>, C<sub>2</sub>H<sub>6</sub>, C<sub>3</sub>H<sub>6</sub>, and C<sub>3</sub>H<sub>4</sub>)

374

remarkably decreases. C<sub>2</sub>H<sub>2</sub> increases mainly from other C<sub>2</sub> conversion [84]. These results

375

confirm that light hydrocarbons are considerably reformed to H<sub>2</sub> and CO in the gasification

376

process when the temperature increases.

377

The carbon atoms distribution shows that the most important species are:

378

CO<sub>2</sub>>CO>C<sub>2</sub>H<sub>4</sub>>CH<sub>4</sub>>C<sub>6</sub>H<sub>6</sub> (Figure 3-B). C<sub>6</sub>H<sub>6</sub> is a stable tertiary product not converted in our

379

conditions [83, 85]. A decrease in CO<sub>2</sub> is observed at 900°C, together with an increase in CO,

380

C<sub>6</sub>H<sub>6</sub>, and CH<sub>4</sub>. These evolutions suggest that dry reforming reactions are promoted at high

381 temperature [86]. The increase in temperature promotes the kinetics of reactions (water gas  
382 shift, hydrocarbons reforming, etc.) but also modifies the thermodynamic equilibrium of the  
383 reactive system. We have previously studied the effect of temperature on the detailed  
384 mechanisms of syngas conversion. We have especially shown that OH radicals are mainly  
385 produced by CO<sub>2</sub> conversion ( $\text{CO}_2 + \text{H} = \text{CO} + \text{OH}$ ) in a syngas [84]. Therefore, under air  
386 gasification conditions, CO<sub>2</sub> yields are controlled by the competition between oxidation  
387 reactions (producing CO<sub>2</sub>) and CO<sub>2</sub> conversion in the gas phase. In comparison with syngas  
388 produced in the same reactor under similar operating conditions with other types of SRF [78],  
389 the syngas produced by this SRF presents a CO<sub>2</sub> and CO contents significantly lower, while  
390 the content in CH<sub>4</sub> and C<sub>2</sub>H<sub>4</sub>, and mainly C<sub>3</sub>H<sub>6</sub> are higher. The low content of CO and CO<sub>2</sub>  
391 results from the low O/C ratio in the plastic contained in SRF, as clearly explained by *Valin et*  
392 *al.* [38]. The high content in C<sub>3</sub>H<sub>6</sub> with this SRF is expected to result from the fast  
393 decomposition of polymer chains of the plastics contained in this SRF, and to the low catalytic  
394 activity of olivine towards tar reforming reactions due to poisoning of active sites with  
395 inorganic gases [55].

### 396 *3.2.2 Influence of the Equivalence Ratio*

397 The evolutions of the gasification indicators with increasing ER are presented in [Table 3](#). It can  
398 be observed that increasing ER results in a decrease of the CGE, a significant increase in syngas  
399 yield, and a drastic drop of the LHV<sub>syngas</sub>. While oxidation reactions are expected to increase  
400 with higher ER, the carbon conversion is almost stable between ER=0.22 and 0.27. The large  
401 amount of inorganic species known for their catalytic activity (such as Ca, Na, K or Fe) could  
402 catalyze the gasification reactions of the carbonaceous solids and promote the carbon  
403 conversion even at low ER [87]. Nevertheless, approximately 10 to 13 wt.% of the carbon  
404 inlet was not converted. Most of this non-converted carbon was supposed to be recovered in  
405 the form of fly ash and tar compounds. The elemental composition of the fly ash was analyzed.

406 Whatever the ER value, it consists mainly in ash (~87 wt.%), carbon (~12 wt.%), low amounts  
407 of hydrogen (~0.7 wt.%) and nitrogen (~0.5 wt.%). During the gasification at 800°C, the fly  
408 ash yield was 16 wt.%. Thus, the fly ash contains 5.5 wt.% of the carbon input. This result  
409 confirms that part of the carbon input is not converted during gasification and is recovered in  
410 the form of fly ash. This results exemplifies the important effect of particles elutriation on the  
411 carbon balance [88].

412 The increase in syngas yield with rising ER is explained by the higher ratio of air to SRF in the  
413 gasifier, leading to a higher dilution of the syngas produced into N<sub>2</sub> from air. To better  
414 understand the effects of increasing ER on the syngas produced, the syngas yield and the  
415 LHV<sub>syngas</sub> have been calculated for N<sub>2</sub>-free syngas (Figure S.2 in Supplementary Material). The  
416 results demonstrate that LHV<sub>syngas</sub> of N<sub>2</sub>-free syngas sharply decreases with increasing ER.  
417 Simultaneously, the syngas yield was shown to be almost invariant with rising ER. As a result,  
418 increasing ER results in the decrease of CGE.

419 Table 3 presents the syngas composition at the gasifier outlet (including N<sub>2</sub>), while Figure S.3  
420 (in supplementary material) displays the composition of the gas produced by gasification  
421 without nitrogen. Rising ER decreases the fraction of the produced gases, except for CO<sub>2</sub> which  
422 is generated by the oxidation reactions promoted by high ER. Indeed, syngas and char can both  
423 be oxidized with increasing ER. The syngas oxidation reactions also explain the decrease of  
424 the LHV<sub>syngas</sub> with rising ER (Figure S.2). The syngas yield is not impacted by the ER variation  
425 under the actual conditions of this study. These trends are similar to that obtained during  
426 miscanthus gasification in the same reactor under similar operating conditions [36].

427 The distribution of hydrogen and carbon atoms in the syngas was also investigated. The results,  
428 presented in Figure 3-C and D, reveal that the distribution is poorly modified with rising ER.  
429 For H atoms distribution, the selectivity in CH<sub>4</sub> and C<sub>6</sub>H<sub>6</sub> slightly increases with rising ER,



430 while that of  $C_3H_6$  and  $C_2H_6$  decreases. Indeed,  $CH_4$  and  $C_6H_6$  are known to be more stable  
431 hydrocarbons than  $C_3H_6$  and  $C_2H_6$  [89, 90]. Regarding the carbon atoms distribution, the main  
432 effect of rising ER consists in increasing the  $CO_2$  selectivity. Thus, hydrocarbon molecules  
433 (notably  $C_2H_4$  and  $C_3H_6$ , based on C atoms molar distribution) seem to be oxidized into  $CO_2$   
434 when the ER increases. The higher increase in  $CO_2$  compared to  $H_2$  (and  $CO$ ) in terms of molar  
435 distribution in C or H atoms shows that higher ER promotes  $CO_2$  (and not  $CO$ ) and that steam  
436 reforming reactions are not significantly promoted by ER under our conditions.

437 Compared with results obtained in the same reactor under similar operating conditions with  
438 other types of SRF [78], higher carbon conversion and LHV were obtained with the present  
439 SRF. As a result, the CGE is higher than that obtained with a SRF rich in paper and another  
440 mostly composed of plastics (SRF1 and SRF2 of the previous article [78]). Thus, the mixture  
441 of soft plastics with ash-containing waste in this SRF seems to promote the gasification  
442 efficiency.

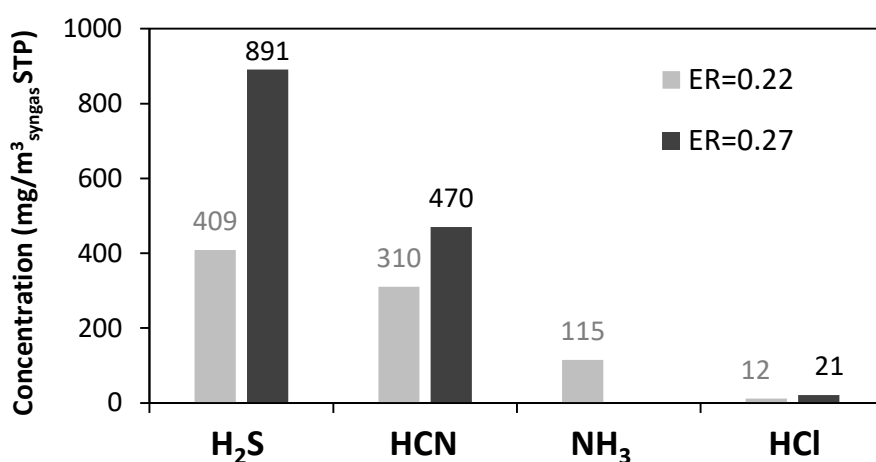
### 443 3.3 Inorganic gases composition

444 As explained in the introduction, conflicting results are presented in the literature about the  
445 effect of ER on the release of inorganic gases. To investigate this phenomenon, the  
446 concentrations of H<sub>2</sub>S, HCl, NH<sub>3</sub> and HCN were measured at two different ER in this study:  
447 0.22 and 0.27. In addition, fly ash and bed material after gasification were analyzed. Since the  
448 solid samples recovered were generated in different operating conditions (constant temperature  
449 but different ER), the results are only qualitative and are presented in supplementary material.

450 The results of inorganic gases analysis (presented in [Figure 4](#)) show that H<sub>2</sub>S is the most  
451 important inorganic gas generated during the gasification of this SRF. Its content increases  
452 from 409 to 891 mg/Nm<sup>3</sup> of syngas with increasing ER. These values correspond respectively  
453 to 11% and 26% of the sulfur contained in the SRF. These values are in agreement with *Pinto*  
454 *et al.* [31], while *Valin et al.* reported that 45 to 65% of sulfur was transformed into H<sub>2</sub>S during  
455 SRF air gasification [38]. To better understand the sulfur species distribution, the sulfur content  
456 of fly ash and bed materials after gasification were qualitatively analyzed in this study  
457 (Supplementary Material). Strong interactions between the olivine bed (containing iron) and  
458 H<sub>2</sub>S are expected to immobilize the produced H<sub>2</sub>S in the fluidized bed during SRF gasification,  
459 while a lower amount of H<sub>2</sub>S seems to be adsorbed on the fly ash due to the presence of AAEM  
460 species and iron. Other species not analyzed in this study, such as tar molecules (thiophene,  
461 benzo- and dibenzo-thiophene, thiols, or aryl and alkyl-sulphides) could also contain part of  
462 the sulfur [31].

463 For nitrogenous gases, both HCN and NH<sub>3</sub> are generated at low ER. However, at ER=0.27, no  
464 ammonia is detected in the syngas, whereas HCN concentration increases. HCN is typically  
465 generated by the decomposition of nitrogenous polymers [61]. The significant plastic content  
466 in this SRF may explain the production of HCN. The NH<sub>3</sub> and HCN contents are in agreement

467 with previous studies dealing with SRF gasification [34, 50, 54], where HCN content was found  
 468 to vary from 27 to 660 mg/Nm<sup>3</sup> and NH<sub>3</sub> from 0 to 200 mg/Nm<sup>3</sup>. Anyway, these HCN and  
 469 NH<sub>3</sub> content correspond to a very small part of the N present in the SRF (less than 6 %). The  
 470 formation of other N-gases (such as N<sub>2</sub>, NO<sub>x</sub>) [39, 57], and condensable compounds (cyano-  
 471 acetylene, acetonitrile, isoquinoline, indole, carbazole, quinoline, other N-heteroaromatic  
 472 compounds) [49, 57, 91, 92] can explain this difference. It should be noted that the formation  
 473 of N<sub>2</sub> is really difficult to assess since it would be highly diluted in the N<sub>2</sub> that comes from air.  
 474 In addition, part of the syngas water could have condensed in the Tedlar bag during sampling,  
 475 possibly leading to NH<sub>3</sub> dissolution [93]. Nevertheless, no trace of condensation was observed  
 476 in the Tedlar bag during experiments. Qualitative distribution of nitrogen compounds presented  
 477 in Supplementary Material highlights that the majority of N-compounds was not identified in  
 478 this study. This issue was also reported by other authors [38].



479

480 **Fig. 4** Influence of the ER on the inorganic gases concentration at T=800°C

481 The content of HCl in the syngas is low compared both to the other inorganic gases and to the  
 482 data available in the literature [30, 54]. This result can be explained by the low Cl content in  
 483 this SRF (0.3 wt.%). But even at ER=0.27, HCl represents less than 2% of the chlorine present  
 484 in the SRF. An explanation is that there are reactions occurring between HCl and the AAEM

485 species of SRF removing HCl from the syngas [68, 94]. The qualitative analysis of fly ash and  
486 bed material presented in Supplementary Material implies that chlorine is mainly trapped in  
487 the fly ash after gasification.

488 These results support the observation of several researchers suggesting that rising ER increases  
489 the inorganic gases content in the syngas [31, 49, 95]. It may be due to the fact that high ER  
490 promotes the char gasification reactions thus enhancing the release of heteroatoms, but in the  
491 results presented in Table 3, the carbon conversion is stable when ER increases from 0.22 to  
492 0.27. This stability is not logical and seems suspicious since rising ER in such a range is  
493 expected to increase the carbon conversion [78]. The values for inorganic gases obtained in  
494 this study are in agreement with the range of available data in the literature [30, 50, 54, 55].

495 The inorganic gases contents are significantly higher than the standard required for syngas  
496 valorization in gas engine. The maximum acceptable values are around 100 mg/m<sup>3</sup> for H<sub>2</sub>S, 50  
497 mg/m<sup>3</sup> for NH<sub>3</sub>, and 9 mg/m<sup>3</sup> for HCl [32, 39]. These results confirm that inorganic gases are  
498 an important issue for the SRF gasification.

#### 499 **4. Conclusions**

500 This article studied air gasification of an industrial Solid Recovered Fuel in allothermal  
501 bubbling fluidized bed. Since the valorization of low-grade SRF by gasification processes  
502 could be jeopardized by the low quality of the resulting syngas, the syngas composition was  
503 deeply analyzed in this study.

504 Increasing gasification temperature from 750 to 800°C had low effect on gasification, while  
505 drastic improvement of gasification efficiency and syngas quality was observed at 900°C. This  
506 beneficial effect was attributed to the promotion of secondary reactions (including  
507 hydrocarbons conversion) and char gasification. The influence of equivalence ratio (ER) was  
508 significantly less important than temperature on the gasification efficiency. The main effect

509 consisted in the decrease of the syngas LHV due to the promotion of oxidation reactions. As a  
510 result, the CO<sub>2</sub> content was found to increase while the CGE decreased.

511 The high content in light hydrocarbon compounds (CH<sub>4</sub>, C<sub>2</sub>H<sub>4</sub>, C<sub>3</sub>H<sub>6</sub>) with this SRF resulted  
512 from the fast decomposition of polymer chains of the plastics contained in this SRF, and to the  
513 low catalytic activity of olivine towards tar reforming reactions due to poisoning of active sites  
514 with inorganic gases (HCl, H<sub>2</sub>S). Compared with results obtained in the same reactor under  
515 similar operating conditions with other types of SRF, the gasification efficiency with the  
516 present SRF was higher than those obtained with a SRF rich in paper and another mostly  
517 composed of plastics. Thus, the mixture of soft plastics with ash-containing waste in this SRF  
518 seems to promote the gasification efficiency.

519 The concentration of H<sub>2</sub>S, HCl, NH<sub>3</sub> and HCN in the syngas produced at 800°C was measured  
520 at two different ER (0.22 and 0.27). Both HCN and NH<sub>3</sub> were generated at low ER. However,  
521 at ER=0.27, no ammonia was recovered in the syngas, whereas HCN concentration increased.  
522 The significant plastic content in this SRF may explain the release of HCN. The nitrogen mass  
523 inventory was low, reflecting that most of nitrogen compounds were not detected in the form  
524 of NH<sub>3</sub> or HCN. The HCl content in syngas was low compared to the data available in the  
525 literature, due to the low Cl content in the SRF (0.3 wt.%) and to the immobilization of Cl in  
526 the fly ash containing K and Ca. H<sub>2</sub>S was the most important inorganic gas and its content  
527 increased with increasing ER : from 409 to 891 mg/m<sup>3</sup> STP at ER=0.22 and 0.27, respectively.  
528 These values correspond to 11% and 26% of the sulfur present in SRF, while part of sulfur was  
529 expected to react with the olivine bed.

530 Even if the S, N and Cl present in the SRF are not converted completely into inorganic gases,  
531 the concentrations of H<sub>2</sub>S, NH<sub>3</sub> and HCl are too high in comparison with the maximum  
532 acceptable values for syngas valorization in gas engine. Qualitative analysis of fly ash and

533 olivine bed after gasification tests proved that interactions between these materials and  
534 inorganic gases occur allowing to limit the inorganic gases production. More work is needed  
535 to deeply understand the exact nature of the gasification products that contained S, N and Cl,  
536 as well as to optimize waste mixture composition in SRF to promote interactions between  
537 inorganic gases and fly ash/bed material in order to limit the presence of inorganic gases in the  
538 gasifier.

## 539 Acknowledgements

540 The authors acknowledge the financial support of ADEME, France –Terracotta project, n°  
541 1606C0013. The authors also thank the EDF Company, France, especially Emmanuel Thunin  
542 and Mathieu Insa for their support on material characterizations, as well as Matthieu Debal,  
543 Pierre Girods and Yann Rogaume (LERMAB, University de Lorraine) for their tremendous  
544 work for SRF pelletization.

## 545 References

- 546 1. Kaza, S., Yao, L., Bhada-Tata, P., Van Woerden, F.: What a waste 2.0: A global Snapshot of Solid  
547 Waste Management to 2050. , Washington, DC (2018)
- 548 2. Kang, P., Zhang, H., Duan, H.: Characterizing the implications of waste dumping surrounding  
549 the Yangtze River economic belt in China. *J. Hazard. Mater.* 383, 121207 (2020).  
550 <https://doi.org/10.1016/j.jhazmat.2019.121207>
- 551 3. Hafeez, S., Mahmood, A., Syed, J.H., Li, J., Ali, U., Malik, R.N., Zhang, G.: Waste dumping sites as  
552 a potential source of POPs and associated health risks in perspective of current waste  
553 management practices in Lahore city, Pakistan. *Sci. Total Environ.* 562, 953–961 (2016).  
554 <https://doi.org/10.1016/j.scitotenv.2016.01.120>
- 555 4. Rego, R.F., Moraes, L.R.S., Dourado, I.: Diarrhoea and garbage disposal in Salvador, Brazil.  
556 *Trans. R. Soc. Trop. Med. Hyg.* 99, 48–54 (2005). <https://doi.org/10.1016/j.trstmh.2004.02.008>
- 557 5. Kupchik, G.J., Franz, G.J.: Solid Waste, Air Pollution and Health. *J. Air Pollut. Control Assoc.* 26,  
558 116–118 (1976). <https://doi.org/10.1080/00022470.1976.10470229>
- 559 6. Triassi, M., Alfano, R., Illario, M., Nardone, A., Caporale, O., Montuori, P., Triassi, M., Alfano, R.,  
560 Illario, M., Nardone, A., Caporale, O., Montuori, P.: Environmental Pollution from Illegal Waste  
561 Disposal and Health Effects: A Review on the “Triangle of Death.” *Int. J. Environ. Res. Public*.  
562 *Health.* 12, 1216–1236 (2015). <https://doi.org/10.3390/ijerph120201216>
- 563 7. Plaza, P.I., Lambertucci, S.A.: How are garbage dumps impacting vertebrate demography,  
564 health, and conservation? *Glob. Ecol. Conserv.* 12, 9–20 (2017).  
565 <https://doi.org/10.1016/j.gecco.2017.08.002>
- 566 8. Schweitzer, L., Noblet, J.: Chapter 3.6 - Water Contamination and Pollution. In: Török, B. and  
567 Dransfield, T. (eds.) *Green Chemistry*. pp. 261–290. Elsevier (2018)
- 568 9. Lebreton, L., Slat, B., Ferrari, F., Sainte-Rose, B., Aitken, J., Marthouse, R., Hajbane, S., Cunsolo,  
569 S., Schwarz, A., Levivier, A., Noble, K., Debeljak, P., Maral, H., Schoeneich-Argent, R., Brambini,  
570 R., Reisser, J.: Evidence that the Great Pacific Garbage Patch is rapidly accumulating plastic. *Sci.*  
571 *Rep.* 8, 4666 (2018). <https://doi.org/10.1038/s41598-018-22939-w>
- 572 10. Haward, M.: Plastic pollution of the world’s seas and oceans as a contemporary challenge in  
573 ocean governance. *Nat. Commun.* 9, 667 (2018). <https://doi.org/10.1038/s41467-018-03104-3>
- 574 11. Solid Waste Management,  
575 <http://www.worldbank.org/en/topic/urbandevelopment/brief/solid-waste-management>
- 576 12. Martignon, G., Edo, M.: Trends on use of solid recovered fuels. IEA Bioenergy (2020)
- 577 13. Vonk, G., Piriou, B., Wolbert, D., Cammarano, C., Vaïtilingom, G.: Analysis of pollutants in the  
578 product gas of a pilot scale downdraft gasifier fed with wood, or mixtures of wood and waste  
579 materials. *Biomass Bioenergy.* 125, 139–150 (2019).  
580 <https://doi.org/10.1016/j.biombioe.2019.04.018>

- 581 14. Combustibles solides de récupération (CSR) - Caractérisation et évaluation de leurs  
582 performances en combustion. FEDEREC et COMPTE-R (2015)
- 583 15. Consommation d'énergie primaire - Eurostat, [https://ec.europa.eu/eurostat/fr/web/products-](https://ec.europa.eu/eurostat/fr/web/products-datasets/-/T2020_33)  
584 [datasets/-/T2020\\_33](https://ec.europa.eu/eurostat/fr/web/products-datasets/-/T2020_33)
- 585 16. Brunner, P.H., Morf, L., Rechberger, H.: VI.3 - Thermal waste treatment – a necessary element  
586 for sustainable waste management. In: Twardowska, I. (ed.) Waste Management Series. pp.  
587 783–806. Elsevier (2004)
- 588 17. Porteous, A.: Why energy from waste incineration is an essential component of  
589 environmentally responsible waste management. *Waste Manag.* 25, 451–459 (2005).  
590 <https://doi.org/10.1016/j.wasman.2005.02.008>
- 591 18. Arena, U.: Process and technological aspects of municipal solid waste gasification. A review.  
592 *Waste Manag.* 32, 625–639 (2012). <https://doi.org/10.1016/j.wasman.2011.09.025>
- 593 19. Enerkem produces renewable alternative solution to diesel fuel. *Focus Catal.* 2018, 6 (2018).  
594 <https://doi.org/10.1016/j.focat.2018.11.097>
- 595 20. Barba, A., Le Cadre, E., Forsgren, H., Gaillard, M., Gunnarsson, I., Guerrini, O., Hoff, M.V., Kara,  
596 Y., Mollema, E., Moretti, I., Ourliac, M., Overwijk, M., Peureux, G., Peltenburg, A., Tengberg, F.,  
597 De Vries, T., Winjstra, S.: Europe move towards industrialization of 2G biomethane from  
598 biomass gasification and methanation. Presented at the International Gas Research  
599 Conference Proceedings (2017)
- 600 21. Ramos, A., Monteiro, E., Silva, V., Rouboa, A.: Co-gasification and recent developments on  
601 waste-to-energy conversion: A review. *Renew. Sustain. Energy Rev.* 81, 380–398 (2018).  
602 <https://doi.org/10.1016/j.rser.2017.07.025>
- 603 22. Sansaniwal, S.K., Pal, K., Rosen, M.A., Tyagi, S.K.: Recent advances in the development of  
604 biomass gasification technology: A comprehensive review. *Renew. Sustain. Energy Rev.* 72,  
605 363–384 (2017). <https://doi.org/10.1016/j.rser.2017.01.038>
- 606 23. Campoy, M., Gómez-Barea, A., Ollero, P., Nilsson, S.: Gasification of wastes in a pilot fluidized  
607 bed gasifier. *Fuel Process. Technol.* 121, 63–69 (2014).  
608 <https://doi.org/10.1016/j.fuproc.2013.12.019>
- 609 24. Karatas, H., Olgun, H., Engin, B., Akgun, F.: Experimental results of gasification of waste tire  
610 with air in a bubbling fluidized bed gasifier. *Fuel.* 105, 566–571 (2013).  
611 <https://doi.org/10.1016/j.fuel.2012.08.038>
- 612 25. Xiao, G., Ni, M.-J., Chi, Y., Cen, K.-F.: Low-temperature gasification of waste tire in a fluidized  
613 bed. *Energy Convers. Manag.* 49, 2078–2082 (2008).  
614 <https://doi.org/10.1016/j.enconman.2008.02.016>
- 615 26. Di Gregorio, F., Santoro, D., Arena, U.: The effect of ash composition on gasification of poultry  
616 wastes in a fluidized bed reactor. *Waste Manag. Res.* 32, 323–330 (2014).  
617 <https://doi.org/10.1177/0734242X14525821>
- 618 27. Mastellone, M.L., Zaccariello, L., Arena, U.: Co-gasification of coal, plastic waste and wood in a  
619 bubbling fluidized bed reactor. *Fuel.* 89, 2991–3000 (2010).  
620 <https://doi.org/10.1016/j.fuel.2010.05.019>
- 621 28. Arena, U., Di Gregorio, F.: Energy generation by air gasification of two industrial plastic wastes  
622 in a pilot scale fluidized bed reactor. *Energy.* 68, 735–743 (2014).  
623 <https://doi.org/10.1016/j.energy.2014.01.084>
- 624 29. Wilk, V., Hofbauer, H.: Co-gasification of Plastics and Biomass in a Dual Fluidized-Bed Steam  
625 Gasifier: Possible Interactions of Fuels. *Energy Fuels.* 27, 3261–3273 (2013).  
626 <https://doi.org/10.1021/ef400349k>
- 627 30. Dunnu, G., Panopoulos, K.D., Karellas, S., Maier, J., Toulou, S., Koufodimos, G., Boukis, I.,  
628 Kakaras, E.: The solid recovered fuel Stabilat®: Characteristics and fluidised bed gasification  
629 tests. *Fuel.* 93, 273–283 (2012). <https://doi.org/10.1016/j.fuel.2011.08.061>
- 630 31. Pinto, F., André, R.N., Carolino, C., Miranda, M., Abelha, P., Direito, D., Perdikaris, N., Boukis, I.:  
631 Gasification improvement of a poor quality solid recovered fuel (SRF). Effect of using natural



- 632 minerals and biomass wastes blends. *Fuel*. 117, 1034–1044 (2014).  
633 <https://doi.org/10.1016/j.fuel.2013.10.015>
- 634 32. Milne, T.A., Evans, R.J., Abatzoglou, N.: Biomass Gasifier Tars: Their Nature, Formation and  
635 Conversion. National Renewable Energy Laboratory (1998)
- 636 33. Vonk, G., Piriou, B., Felipe Dos Santos, P., Wolbert, D., Vaïtilingom, G.: Comparative analysis of  
637 wood and solid recovered fuels gasification in a downdraft fixed bed reactor. *Waste Manag.*  
638 85, 106–120 (2019). <https://doi.org/10.1016/j.wasman.2018.12.023>
- 639 34. Arena, U., Di Gregorio, F.: Gasification of a solid recovered fuel in a pilot scale fluidized bed  
640 reactor. *Fuel*. 117, 528–536 (2014). <https://doi.org/10.1016/j.fuel.2013.09.044>
- 641 35. Recari Ansa, J.: Gasification of biomass and solid recovered fuels (SRFs) for the synthesis of  
642 liquid fuels, (2017)
- 643 36. Lardier, G., Kaknics, J., Dufour, A., Michel, R., Cluet, B., Authier, O., Poirier, J., Mauviel, G.: Gas  
644 and Bed Axial Composition in a Bubbling Fluidized Bed Gasifier: Results with Miscanthus and  
645 Olivine. *Energy Fuels*. 30, 8316–8326 (2016). <https://doi.org/10.1021/acs.energyfuels.6b01816>
- 646 37. Horvat, A., Kwapinska, M., Xue, G., Rabou, L.P.L.M., Pandey, D.S., Kwapinski, W., Leahy, J.J.:  
647 Tars from Fluidized Bed Gasification of Raw and Torrefied Miscanthus x giganteus. *Energy*  
648 *Fuels*. 30, 5693–5704 (2016). <https://doi.org/10.1021/acs.energyfuels.6b00532>
- 649 38. Valin, S., Ravel, S., Pons de Vincent, P., Thiery, S., Miller, H.: Fluidized bed air gasification of  
650 solid recovered fuel and woody biomass: Influence of experimental conditions on product gas  
651 and pollutant release. *Fuel*. 242, 664–672 (2019). <https://doi.org/10.1016/j.fuel.2019.01.094>
- 652 39. Woolcock, P.J., Brown, R.C.: A review of cleaning technologies for biomass-derived syngas.  
653 *Biomass Bioenergy*. 52, 54–84 (2013). <https://doi.org/10.1016/j.biombioe.2013.02.036>
- 654 40. Torres, W., Pansare, S.S., Jr, J.G.G.: Hot Gas Removal of Tars, Ammonia, and Hydrogen Sulfide  
655 from Biomass Gasification Gas. *Catal. Rev.* 49, 407–456 (2007).  
656 <https://doi.org/10.1080/01614940701375134>
- 657 41. Asadullah, M.: Biomass gasification gas cleaning for downstream applications: A comparative  
658 critical review. *Renew. Sustain. Energy Rev.* 40, 118–132 (2014).  
659 <https://doi.org/10.1016/j.rser.2014.07.132>
- 660 42. GE Jenbacher: Fuel gas quality, special gases. (2009)
- 661 43. Gupta, R.P., Turk, B.S., Portzer, J.W., Cicero, D.C.: Desulfurization of syngas in a transport  
662 reactor. *Environ. Prog.* 20, 187–195 (2001)
- 663 44. Lee, J., Feng, B.: A thermodynamic study of the removal of HCl and H<sub>2</sub>S from syngas. *Front.*  
664 *Chem. Sci. Eng.* 6, 67–83 (2012). <https://doi.org/10.1007/s11705-011-1162-4>
- 665 45. Tijmensen, M.J.A., Faaij, A.P.C., Hamelinck, C.N., van Hardeveld, M.R.M.: Exploration of the  
666 possibilities for production of Fischer Tropsch liquids and power via biomass gasification.  
667 *Biomass Bioenergy*. 23, 129–152 (2002). [https://doi.org/10.1016/S0961-9534\(02\)00037-5](https://doi.org/10.1016/S0961-9534(02)00037-5)
- 668 46. Chiche, D., Diverchy, C., Lucquin, A.-C., Porcheron, F., Defoort, F.: Synthesis Gas Purification. *Oil*  
669 *Gas Sci. Technol. – Rev. D’IFP Energ. Nouv.* 68, 707–723 (2013).  
670 <https://doi.org/10.2516/ogst/2013175>
- 671 47. Kaufman Rechulski, M.D., Schildhauer, T.J., Biollaz, S.M.A., Ludwig, Ch.: Sulfur containing  
672 organic compounds in the raw producer gas of wood and grass gasification. *Fuel*. 128, 330–339  
673 (2014). <https://doi.org/10.1016/j.fuel.2014.02.038>
- 674 48. Arena, U., Di Gregorio, F.: Fluidized bed gasification of industrial solid recovered fuels. *Waste*  
675 *Manag.* 50, 86–92 (2016). <https://doi.org/10.1016/j.wasman.2016.02.011>
- 676 49. Wilk, V., Hofbauer, H.: Conversion of fuel nitrogen in a dual fluidized bed steam gasifier. *Fuel*.  
677 106, 793–801 (2013). <https://doi.org/10.1016/j.fuel.2012.12.056>
- 678 50. Berruoco, C., Recari, J., Abelló, S., Farriol, X., Montané, D.: Experimental Investigation of Solid  
679 Recovered Fuel (SRF) Gasification: Effect of Temperature and Equivalence Ratio on Process  
680 Performance and Release of Minor Contaminants. *Energy Fuels*. 29, 7419–7427 (2015).  
681 <https://doi.org/10.1021/acs.energyfuels.5b02032>

- 682 51. Berruenco, C., Recari, J., Güell, B.M., Alamo, G. del: Pressurized gasification of torrefied woody  
683 biomass in a lab scale fluidized bed. *Energy*. 70, 68–78 (2014).  
684 <https://doi.org/10.1016/j.energy.2014.03.087>
- 685 52. Gas analysis in gasification of biomass and waste - Guideline report Document 1. IEA Bioenergy  
686 Task 33 (2018)
- 687 53. Aljbour, S.H., Kawamoto, K.: Bench-scale gasification of cedar wood – Part II: Effect of  
688 Operational conditions on contaminant release. *Chemosphere*. 90, 1501–1507 (2013).  
689 <https://doi.org/10.1016/j.chemosphere.2012.08.030>
- 690 54. Recari, J., Berruenco, C., Abelló, S., Montané, D., Farriol, X.: Gasification of two solid recovered  
691 fuels (SRFs) in a lab-scale fluidized bed reactor: Influence of experimental conditions on  
692 process performance and release of HCl, H<sub>2</sub>S, HCN and NH<sub>3</sub>. *Fuel Process. Technol.* 142, 107–  
693 114 (2016). <https://doi.org/10.1016/j.fuproc.2015.10.006>
- 694 55. Arena, U., Zaccariello, L., Mastellone, M.L.: Fluidized bed gasification of waste-derived fuels.  
695 *Waste Manag.* 30, 1212–1219 (2010). <https://doi.org/10.1016/j.wasman.2010.01.038>
- 696 56. Pels, J.R., Kapteijn, F., Moulijn, J.A., Zhu, Q., Thomas, K.M.: Evolution of nitrogen functionalities  
697 in carbonaceous materials during pyrolysis. *Carbon*. 33, 1641–1653 (1995).  
698 [https://doi.org/10.1016/0008-6223\(95\)00154-6](https://doi.org/10.1016/0008-6223(95)00154-6)
- 699 57. Leppälahti, J., Koljonen, T.: Nitrogen evolution from coal, peat and wood during gasification:  
700 Literature review. *Fuel Process. Technol.* 43, 1–45 (1995). [https://doi.org/10.1016/0378-3820\(94\)00123-B](https://doi.org/10.1016/0378-3820(94)00123-B)
- 702 58. Leppälahti, J., Kurkela, E.: Behaviour of nitrogen compounds and tars in fluidized bed air  
703 gasification of peat. *Fuel*. 70, 491–497 (1991). [https://doi.org/10.1016/0016-2361\(91\)90026-7](https://doi.org/10.1016/0016-2361(91)90026-7)
- 704 59. Hansson, K.-M., Samuelsson, J., Tullin, C., Åmand, L.-E.: Formation of HNCO, HCN, and NH<sub>3</sub>  
705 from the pyrolysis of bark and nitrogen-containing model compounds. *Combust. Flame*. 137,  
706 265–277 (2004). <https://doi.org/10.1016/j.combustflame.2004.01.005>
- 707 60. Kelemen, S.R., Afeworki, M., Gorbaty, M.L., Kwiatek, P.J., Sansone, M., Walters, C.C., Cohen,  
708 A.D.: Thermal Transformations of Nitrogen and Sulfur Forms in Peat Related to Coalification.  
709 *Energy Fuels*. 20, 635–652 (2006). <https://doi.org/10.1021/ef050307p>
- 710 61. Leichtnam, J., Schwartz, D., Gadiou, R.: The behaviour of fuel-nitrogen during fast pyrolysis of  
711 polyamide at high temperature. *J. Anal. Appl. Pyrolysis*. 55, 255 (2000)
- 712 62. Scott, D.S., Piskorz, J.: The continuous flash pyrolysis of biomass. *Can. J. Chem. Eng.* 62, 404–  
713 412 (1984). <https://doi.org/10.1002/cjce.5450620319>
- 714 63. Scott, D.S., Piskorz, J., Westerberg, I.B., McKeough, P.: Flash pyrolysis of peat in a fluidized bed.  
715 *Fuel Process. Technol.* 18, 81–95 (1988). [https://doi.org/10.1016/0378-3820\(88\)90076-8](https://doi.org/10.1016/0378-3820(88)90076-8)
- 716 64. Tian, F.-J., Yu, J., McKenzie, L.J., Hayashi, J., Li, C.-Z.: Conversion of Fuel-N into HCN and NH<sub>3</sub>  
717 During the Pyrolysis and Gasification in Steam: A Comparative Study of Coal and Biomass.  
718 *Energy Fuels*. 21, 517–521 (2007). <https://doi.org/10.1021/ef060415r>
- 719 65. Kurkela, E., Laatikainen, J., Ståhlberg, P.: Pressurized Fluidized-bed Gasification Experiments  
720 with Wood, Peat and Coal at VTT in 1991-1992: Gasification of danish wheat straw and coal.  
721 VTT (1996)
- 722 66. Glarborg, P., Jensen, A.D., Johnsson, J.E.: Fuel nitrogen conversion in solid fuel fired systems.  
723 *Prog. Energy Combust. Sci.* 29, 89–113 (2003). [https://doi.org/10.1016/S0360-1285\(02\)00031-X](https://doi.org/10.1016/S0360-1285(02)00031-X)
- 724 X
- 725 67. Ma, W., Hoffmann, G., Schirmer, M., Chen, G., Rotter, V.S.: Chlorine characterization and  
726 thermal behavior in MSW and RDF. *J. Hazard. Mater.* 178, 489–498 (2010).  
727 <https://doi.org/10.1016/j.jhazmat.2010.01.108>
- 728 68. Bläsing, M., Zini, M., Müller, M.: Influence of Feedstock on the Release of Potassium, Sodium,  
729 Chlorine, Sulfur, and Phosphorus Species during Gasification of Wood and Biomass Shells.  
730 *Energy Fuels*. 27, 1439–1445 (2013). <https://doi.org/10.1021/ef302093r>

- 731 69. Corella, J., Toledo, J.M., Molina, G.: Performance of CaO and MgO for the hot gas clean up in  
732 gasification of a chlorine-containing (RDF) feedstock. *Bioresour. Technol.* 99, 7539–7544  
733 (2008). <https://doi.org/10.1016/j.biortech.2008.02.018>
- 734 70. Lu, H., Purushothama, S., Hyatt, J., Pan, W.-P., Riley, J.T., Lloyd, W.G., Flynn, J., Gill, P.: Co-firing  
735 high-sulfur coals with refuse-derived fuel. *Thermochim. Acta.* 284, 161–177 (1996).  
736 [https://doi.org/10.1016/0040-6031\(96\)02864-X](https://doi.org/10.1016/0040-6031(96)02864-X)
- 737 71. Jazbec, M., Sendt, K., Haynes, B.S.: Kinetic and thermodynamic analysis of the fate of sulphur  
738 compounds in gasification products. *Fuel.* 83, 2133–2138 (2004).  
739 <https://doi.org/10.1016/j.fuel.2004.06.017>
- 740 72. Tchapda, A., Pisupati, S., Tchapda, A.H., Pisupati, S.V.: A Review of Thermal Co-Conversion of  
741 Coal and Biomass/Waste. *Energies.* 7, 1098–1148 (2014). <https://doi.org/10.3390/en7031098>
- 742 73. Knudsen, J.N., Jensen, P.A., Lin, W., Frandsen, F.J., Dam-Johansen, K.: Sulfur Transformations  
743 during Thermal Conversion of Herbaceous Biomass. *Energy Fuels.* 18, 810–819 (2004).  
744 <https://doi.org/10.1021/ef034085b>
- 745 74. Hervy, M., Pham Minh, D., Gérente, C., Weiss-Hortala, E., Nzihou, A., Villot, A., Le Coq, L.: H<sub>2</sub>S  
746 removal from syngas using wastes pyrolysis chars. *Chem. Eng. J.* 334, 2179–2189 (2018).  
747 <https://doi.org/10.1016/j.cej.2017.11.162>
- 748 75. Broer, K.M., Brown, R.C.: The role of char and tar in determining the gas-phase partitioning of  
749 nitrogen during biomass gasification. *Appl. Energy.* 158, 474–483 (2015).  
750 <https://doi.org/10.1016/j.apenergy.2015.08.100>
- 751 76. Pinto, F., Lopes, H., André, R.N., Gulyurtlu, I., Cabrita, I.: Effect of catalysts in the quality of  
752 syngas and by-products obtained by co-gasification of coal and wastes. 1. Tars and nitrogen  
753 compounds abatement. *Fuel.* 86, 2052–2063 (2007).  
754 <https://doi.org/10.1016/j.fuel.2007.01.019>
- 755 77. de Almeida, V.F., Gómez-Barea, A., Arroyo-Caire, J., Pardo, I.: On the Measurement of the Main  
756 Inorganic Contaminants Derived from Cl, S and N in Simulated Waste-Derived Syngas. *Waste*  
757 *Biomass Valorization.* (2020). <https://doi.org/10.1007/s12649-019-00879-4>
- 758 78. Hervy, M., Remy, D., Dufour, A., Mauviel, G.: Air-blown gasification of Solid Recovered Fuels  
759 (SRFs) in lab-scale bubbling fluidized-bed-Influence of the operating conditions and of the SRF  
760 composition. *Energy Convers. Manag.* 181, 584–592
- 761 79. Cluet, B., Mauviel, G., Rogaume, Y., Authier, O., Delebarre, A.: Segregation of wood particles in  
762 a bubbling fluidized bed. *Fuel Process. Technol.* 133, 80–88 (2015).  
763 <https://doi.org/10.1016/j.fuproc.2014.12.045>
- 764 80. Blanco, P.H., Wu, C., Onwudili, J.A., Williams, P.T.: Characterization of Tar from the  
765 Pyrolysis/Gasification of Refuse Derived Fuel: Influence of Process Parameters and Catalysis.  
766 *Energy Fuels.* 26, 2107–2115 (2012). <https://doi.org/10.1021/ef300031j>
- 767 81. Morin, M., Nitsch, X., Hémati, M.: Interactions between char and tar during the steam  
768 gasification in a fluidized bed reactor. *Fuel.* 224, 600–609 (2018).  
769 <https://doi.org/10.1016/j.fuel.2018.03.050>
- 770 82. Dufour, A., Masson, E., Girods, P., Rogaume, Y., Zoulalian, A.: Evolution of Aromatic Tar  
771 Composition in Relation to Methane and Ethylene from Biomass Pyrolysis-Gasification. *Energy*  
772 *Fuels.* 25, 4182–4189 (2011). <https://doi.org/10.1021/ef200846g>
- 773 83. Dufour, A., Girods, P., Masson, E., Rogaume, Y., Zoulalian, A.: Synthesis gas production by  
774 biomass pyrolysis: Effect of reactor temperature on product distribution. *Int. J. Hydrog. Energy.*  
775 34, 1726–1734 (2009). <https://doi.org/10.1016/j.ijhydene.2008.11.075>
- 776 84. Dufour, A., Valin, S., Castelli, P., Thiery, S., Boissonnet, G., Zoulalian, A., Glaude, P.-A.:  
777 Mechanisms and Kinetics of Methane Thermal Conversion in a Syngas. *Ind. Eng. Chem. Res.* 48,  
778 6564–6572 (2009). <https://doi.org/10.1021/ie900343b>
- 779 85. Jess, A.: Mechanisms and kinetics of thermal reactions of aromatic hydrocarbons from  
780 pyrolysis of solid fuels. *Fuel.* 75, 1441–1448 (1996). [https://doi.org/10.1016/0016-](https://doi.org/10.1016/0016-2361(96)00136-6)  
781 [2361\(96\)00136-6](https://doi.org/10.1016/0016-2361(96)00136-6)

- 782 86. Phan, T.S., Sane, A.R., Rêgo de Vasconcelos, B., Nzihou, A., Sharrock, P., Grouset, D., Pham  
783 Minh, D.: Hydroxyapatite supported bimetallic cobalt and nickel catalysts for syngas production  
784 from dry reforming of methane. *Appl. Catal. B Environ.* 224, 310–321 (2018).  
785 <https://doi.org/10.1016/j.apcatb.2017.10.063>
- 786 87. Dupont, C., Jacob, S., Marrakchy, K.O., Hognon, C., Grateau, M., Labalette, F., Da Silva Perez,  
787 D.: How inorganic elements of biomass influence char steam gasification kinetics. *Energy*. 109,  
788 430–435 (2016). <https://doi.org/10.1016/j.energy.2016.04.094>
- 789 88. Bates, R.B., Altantzis, C., Ghoniem, A.F.: Modeling of Biomass Char Gasification, Combustion,  
790 and Attrition Kinetics in Fluidized Beds. *Energy Fuels*. 30, 360–376 (2016).  
791 <https://doi.org/10.1021/acs.energyfuels.5b02120>
- 792 89. Westbrook, C.K., Dryer, F.L.: Chemical kinetic modeling of hydrocarbon combustion. *Prog.*  
793 *Energy Combust. Sci.* 10, 1–57 (1984). [https://doi.org/10.1016/0360-1285\(84\)90118-7](https://doi.org/10.1016/0360-1285(84)90118-7)
- 794 90. Battin-Leclerc, F.: Detailed chemical kinetic models for the low-temperature combustion of  
795 hydrocarbons with application to gasoline and diesel fuel surrogates. *Prog. Energy Combust.*  
796 *Sci.* 34, 440–498 (2008). <https://doi.org/10.1016/j.peccs.2007.10.002>
- 797 91. Debono, O., Villot, A.: Nitrogen products and reaction pathway of nitrogen compounds during  
798 the pyrolysis of various organic wastes. *J. Anal. Appl. Pyrolysis*. 114, 222–234 (2015).  
799 <https://doi.org/10.1016/j.jaap.2015.06.002>
- 800 92. Chen, H., Wang, Y., Xu, G., Yoshikawa, K.: Fuel-N Evolution during the Pyrolysis of Industrial  
801 Biomass Wastes with High Nitrogen Content. *Energies*. 5, 5418–5438 (2012).  
802 <https://doi.org/10.3390/en5125418>
- 803 93. Recari, J., Berruero, C., Abelló, S., Montané, D., Farriol, X.: Effect of Bed Material on  
804 Oxygen/Steam Gasification of Two Solid Recovered Fuels (SRFs) in a Bench-Scale Fluidized-Bed  
805 Reactor. *Energy Fuels*. 31, 8445–8453 (2017).  
806 <https://doi.org/10.1021/acs.energyfuels.7b01507>
- 807 94. Ephraim, A., Ngo, L., Pham Minh, D., Lebonnois, D., Peregrina, C., Sharrock, P., Nzihou, A.:  
808 Valorization of Waste-Derived Inorganic Sorbents for the Removal of HCl in Syngas. *Waste*  
809 *Biomass Valorization*. (2018). <https://doi.org/10.1007/s12649-018-0355-1>
- 810 95. Delgado, J., Aznar, M.P., Corella, J.: Biomass Gasification with Steam in Fluidized Bed:  
811 Effectiveness of CaO, MgO, and CaO–MgO for Hot Raw Gas Cleaning. *Ind. Eng. Chem. Res.* 36,  
812 1535–1543 (1997). <https://doi.org/10.1021/ie960273w>
- 813